

MINERALOGICAL ZONATION AND RADIOCHRONOLOGICAL RELATIONS IN A LARGE SULFIDE CHIMNEY FROM THE EAST PACIFIC RISE AT 18°25' S

VESNA MARCHIG AND HEINRICH RÖSCH

Bundesanstalt für Geowissenschaften und Rohstoffe, Alfred-Bentz Haus, Postfach 510153, 3000 Hannover 51, Germany

CLAUDE LALOU AND EVELYNE BRICHET

Centre des Faibles Radioactivités, Laboratoire mixte CNRS-CEA, Domaine du CNRS, 91198 Gif sur Yvette Cedex, France

ELISABETH OUDIN

Bureau de Recherches Géologiques et Minières, BP 6009, 45060 Orléans Cedex, France

ABSTRACT

The top meter of a large, inactive sulfide chimney from a hydrothermal field in the central graben of the East Pacific Rise at 18°25' S has been investigated using mineralogical, geochemical and ²¹⁰Pb/Pb dating methods. Four main mineralization stages have been identified: the oldest, dominated by iron sulfides, produced a massive wall thought to have been precipitated from hydrothermal solutions of the black-smoker type during a short, high-temperature event, as is suggested by remnants of fine-grained pyrrhotite which displays quench textures. This pyrrhotite was replaced by low-temperature colloform pyrite. The massive wall is at least ~60–80 years older than the youngest chimney zone. The next zone, which occupies the central conduit of the initial chimney, was filled ~60–70 years after the massive wall was formed. Hydrothermal solutions discharging through the conduit were protected from seawater and therefore were not quenched. Stoichiometric chalcopyrite, the main component of this zone, may have precipitated in equilibrium with these hydrothermal solutions. The last mineralization stage is due to a less intense reactivation of the system, 0–10 years after the preceding one. During this last stage, the solution was forced through the base of the chimney and migrated upward along the chimney. Thereafter, the chimney was exposed to seawater alteration. A comparison with other EPR chimney-growth models shows that the main mineralogical difference is the absence of barite, and that recrystallization is particularly well-developed, whereas dissolution and replacement, characteristic of the thin black-smoker walls, are not intense. From age determinations, as well as chemical and mineralogical studies, it is concluded that the hydrothermal activity is either a continuous process with cyclical maxima of activity, or a discontinuous process.

Keywords: hydrothermal sulfides, chimney mineralogy and chemistry, ²¹⁰Pb/Pb dating, East Pacific Rise.

SOMMAIRE

Une grande cheminée en sulfure, inactive au moment du prélèvement, provenant d'un champ hydrothermal de la vallée centrale de la dorsale Est-Pacifique (EPR), à 18°25' S, a été étudiée le long de son premier mètre supérieur en utilisant des méthodes minéralogique, géochimique et de data-

tion par la méthode ²¹⁰Pb/Pb. Quatre zones minéralogiques principales ont été identifiées: la plus ancienne, formée essentiellement de sulfures de fer, est une paroi massive qui aurait précipité à partir d'une solution hydrothermale de type fumeur noir lors d'un court événement à haute température, comme l'indiquent des reliquats de pyrrhotite à grains fins qui montrent des textures de trempe. Cette pyrrhotite a été remplacée par de la pyrite colloforme de basse température. La paroi massive est au minimum ~60–80 ans plus vieille que la zone la plus jeune de la cheminée. La zone suivante, qui occupe le conduit central de la cheminée initiale, a été formée ~60–70 ans après la formation de la paroi massive. Les solutions hydrothermales passant dans ce conduit ont été protégées du contact avec l'eau de mer et n'ont par conséquent pas subi de trempe. La chalcopyrite stoechiométrique, composante principale de cette zone, peut avoir précipité en équilibre avec ces solutions hydrothermales. Le dernier stade de minéralisation est dû à une réactivation moins intense du système, 0–10 ans après le précédent. Pendant ce stade, la solution a dû traverser la base de l'édifice et migrer le long de la paroi externe de la cheminée. Enfin, la cheminée a été exposée à l'altération par l'eau de mer. Une comparaison avec les autres modèles de croissance de cheminées de l'EPR montre que la principale différence minéralogique est l'absence de barytine, et que la recristallisation est particulièrement bien développée, tandis que les dissolutions et remplacements caractéristiques des parois des fumeurs noirs ne sont pas intenses. À la lumière des âges, de la minéralogie et de la chimie, nous pensons que l'activité hydrothermale a été soit continue avec des paroxysmes d'intensité cycliques, soit discontinue.

Mots-clés: dorsale Est-Pacifique, sulfures hydrothermaux, minéralogie, chimie des cheminées, datations par ²¹⁰Pb/Pb.

INTRODUCTION

Following the discovery of low-temperature hydrothermal activity at the Galapagos Spreading Center (Corliss & Ballard 1977), fossil polymetallic sulfide edifices were found on the East Pacific Rise (EPR) near 21°N (Francheteau *et al.* 1979). Active, high-temperature black smokers were finally observed during ALVIN dives on the EPR at 21°N

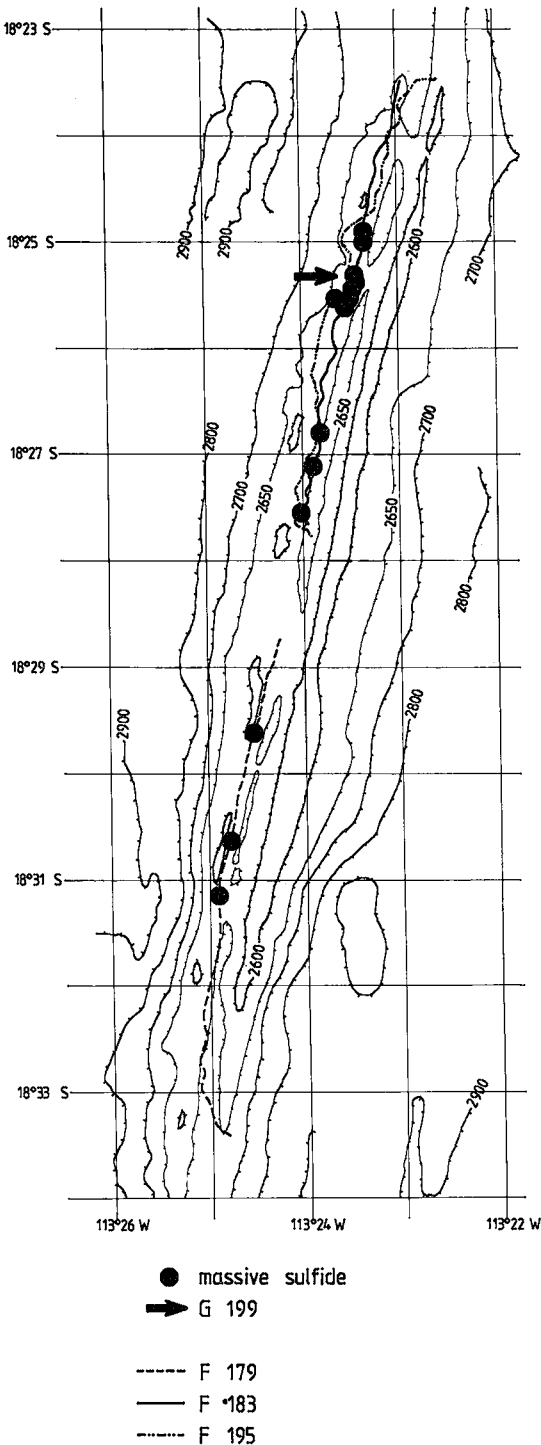
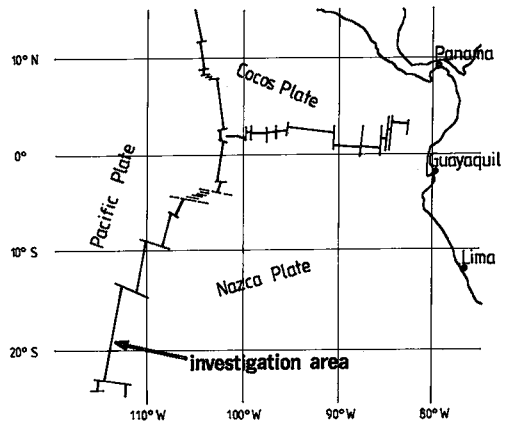


FIG. 1. Map of the EPR near 18°25'S, showing location of main massive sulfide deposits. Contour lines are based on Sea Beam mapping during the SO 40 cruise. Areas above 2600 m are shaded. Note the near-



continuous central graben within the central ridge. F 179, 193 and 195 are tracks of deep-sea camera and instrument tows. The position of the chimney studied in this paper is marked by the arrow (station G 199, at 10°25'S, 113°23'W; water depth 2627 m). Above is a general map of the EPR showing the position of the area investigated.

(RISE Project Group 1980). Such active systems now have been found along the EPR near 12°50' (Hékinian *et al.* 1983), 20°S (Francheteau & Ballard 1983), between 18° and 22°S (Bäcker *et al.* 1985, Tufar *et al.* 1984, 1986), 17°30' to 21°30'S (Renard *et al.* 1985), along the Juan de Fuca Ridge (Normark *et al.* 1983), Endeavor Ridge (Tivey & Delaney 1986), in the Guaymas Basin (Lonsdale *et al.* 1980, Becker & Lonsdale 1985), and, more unexpectedly, on the slowly spreading Mid-Atlantic Ridge (Rona *et al.* 1986).

The present study reports mineralogical and chronological details for a large sample from a massive sulfide chimney near 18°25'S on the EPR. This chimney fragment was recovered during cruise SO 40 of the R/V SONNE, as a part of the GEOMETEP 4 program. The sample displays well-developed growth structures and mineralogical zonation. Consequently, we have tried to establish the links between the nature and duration of hydrothermal activity, and the resulting mineralogical stages of chimney development.

GEOLOGIC SETTING AND SAMPLE DESCRIPTION

The tectonic and geological setting of hydrothermal fields investigated during the SO 40 cruise is described in Marchig & Gundlach (1987) and Marchig *et al.* (1988). Therefore we describe here only the hydrothermal field from which the massive sulfide chimney was sampled, and the setting of the chimney itself. The EPR at the sampling locality displays a ridge with a central graben (Fig. 1). The

eastern walls of the graben are steeper than the western ones, and the bottom of the graben is crossed with fissures and cracks. Hydrothermal indications in the form of yellow hydrothermal sediment and concentrations of fauna are frequent along a 18-km section of the central graben, and massive sulfides are common (Fig. 1). The sample studied here was recovered from the northernmost and largest hydrothermal field.

Sampling of the massive sulfide chimney (Fig. 2) was monitored by a black-and-white television tape. The sample, which represents the top meter of the chimney, weighs about 500 kg and is 40 to 70 cm in diameter. The chimney extends from a single block of massive sulfides, not a mound of broken and partly oxidized chimney fragments as is generally the case. This block also supports another smaller chimney. The top of the chimney was about 10 m above the basaltic basement. Massive sulfides have a dark appearance and a *ruffled* surface (caused by embedded worm tubes), but did not display any living fauna. The two chimneys were not hydrothermally active at the time of sampling, although light-colored sediments, 10–30 cm thick, extended up to 70 m from the sulfide edifice, beyond which were lobate sheet flows of basalt. Sea-anemones grew on the sediment, which locally displayed very light, bioturbated patches, and on the surrounding basalts. Other investigations (Marchig & Gundlach 1987, Marchig *et al.* 1988) indicated that the light-colored sediment is of hydrothermal origin. This sediment consists of bright yellow iron silicate, the surface of which darkens upon ageing. The original yellow color can then be observed only in patches where bioturbation has transported sediment to the surface.

The chimney sample contains an open irregular feeder channel several cm in diameter. The chimney was cut in several slices perpendicular to the direction of this channel. The results described here are for two of these slices (Figs. 3a,b). The megascopic zonation is as follows: i) zone A: a porous outer rim of irregular thickness characterized by alternating whitish and dark grey zones. Holes formed by worm tubes are present mainly in this zone; ii) zone B: massive dark grey sulfides with low porosity and a homogeneous appearance; iii) zone C: feeder channels. In the lower slice, traces of two largely filled feeder channels are visible (C and C'). Relative to zone B, these fills are inhomogeneous and less compact; the fills vary from dark grey to reddish yellow and contain crystals of variable sizes; iv) zone D: black dendritic overgrowths, observed only in the upper slice. These overgrowths are present within cavities in zone C, as well as in worm-tube cavities in zone A. As can be seen in Figure 3c, the zone boundaries are diffuse, especially between zones A and B, perhaps suggestive of continuous or overlapping growth processes.

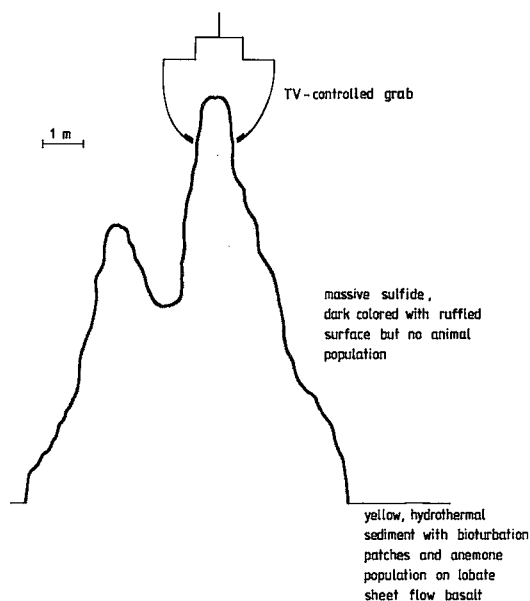


FIG. 2. Sketch of the massive sulfide chimney (station G 199), the top of which was sampled by means of a TV-controlled grab. The sketch is based on videotape footage recorded during sampling.

METHODS

Sampling

Samples were removed from the different mineralogical zones in the chimney using dental drilling equipment. Larger samples for radiochronological study were taken from the lower slice with a hand-drill equipped with a tungsten-carbide bit 7 mm in diameter. Chemical and mineralogical investigations were performed in detail on the upper slice, and also on the lower slice following radiochronological sampling.

Mineralogical and chemical methods

Powdered samples were examined by X-ray diffractometry (XRD) using Cu radiation and a wide-angle goniometer with a graphite monochromator. The same powders were then analyzed chemically using 200 mg of sample which were dissolved in 100 ml of hot 1:1 HNO₃. The undissolved residue was separated from the solution by filtering, was ignited in a Pt crucible, and weighed. The powder was then evaporated three times to dryness with HF, ignited again, and reweighed. The difference between the two weighings represents the SiO₂ content of the sample. Any residue remaining after the HF treatment was dissolved with a small amount of K₂S₂O₇, and was added to the primary solution. The accuracy of this method for silica determination is better than 1%.

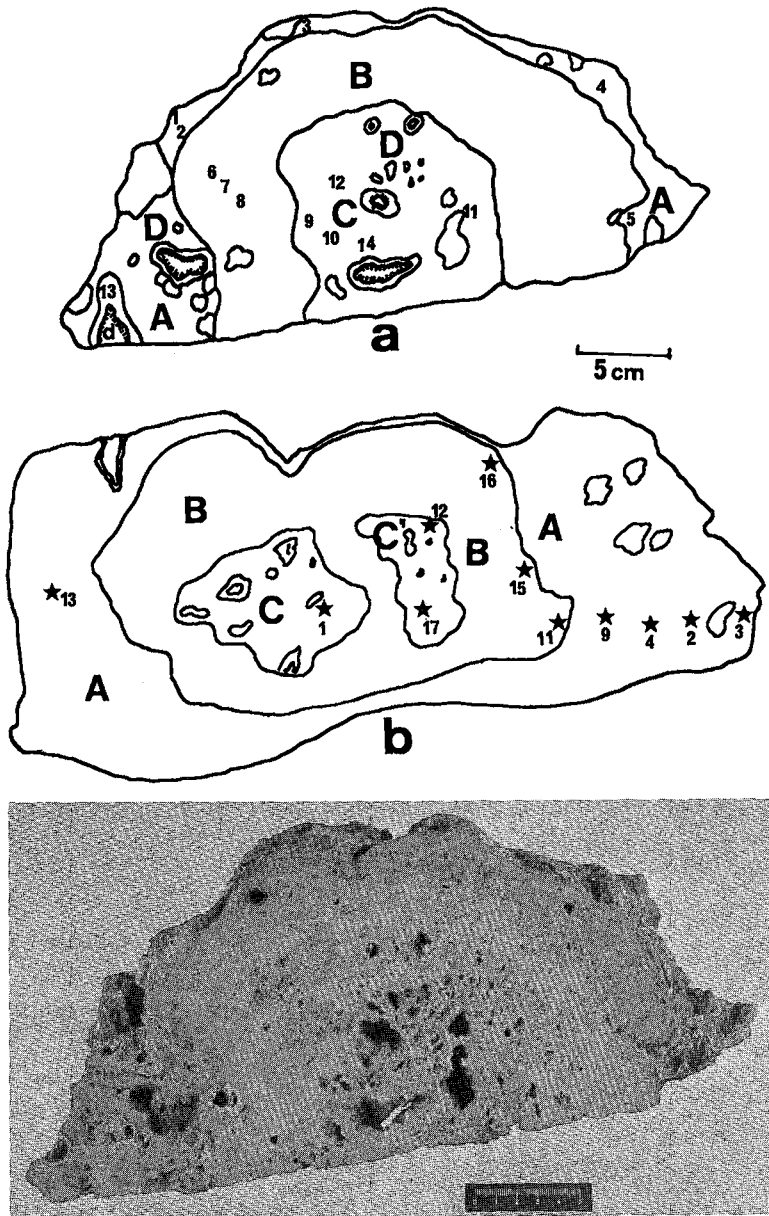


FIG. 3. Sketch of the two massive sulfide slices a) 5 cm from top of chimney; b) 70 cm from the top; c) photograph of the upper slice; bar scale in cm. Most mineralogical and chemical studies were performed on the upper slice, and the radiochronological study on the lower slice. The numbers give samples sites; the letters indicate the main mineral zones.

Fe, Cu, Zn, Ni, Pb, Co, Mn, Mg, Cd and Ag were determined by atomic absorption using an acetylene/air flame, and Al and Mo were determined using an acetylene/N₂O flame. Accuracy checks by analyzing international standards gave agreements better than 5%.

Principle of the ²¹⁰Pb/^{Pb} dating method

During the convective cycle of seawater in hydrothermal systems at mid-ocean ridges, hot and acidic solutions are produced which can leach significant quantities of elements from the basaltic crust (Edmond *et al.* 1979). Among these elements, lead

is of major interest in the establishment of a time scale. Stable lead, and also ^{210}Pb with a radioactive half-life of 22 years, are present in the fluid. When sulfides precipitate from solution, ^{210}Pb and stable Pb are incorporated without fractionation in the sulfide. Lead is present in the sulfides either as a main constituent in galena and lead sulfosalts or, more generally, as impurities in other sulfide minerals (Haymon & Kastner 1981, Oudin 1981, Koski *et al.* 1984). Once in the crystal structure, and in the absence of any exchange, the ^{210}Pb activity decreases, and consequently the lead specific activity (dpm $^{210}\text{Pb}/\mu\text{g}$ of stable lead). Age therefore may be deduced from the equation: $A = A_0 e^{-\lambda t}$ where A_0 is the $^{210}\text{Pb}/\text{Pb}$ ratio at the time of deposition, A is the measured $^{210}\text{Pb}/\text{Pb}$ ratio, and λ is the decay constant of ^{210}Pb .

TABLE 1. MINERALOGICAL COMPOSITION OF THE FOUR GROWTH ZONES*

1996	main components	minor components	traces
Zone A			
1	marcasite	pyrite, sphalerite	jarosite
2	sphalerite, pyrite		chalcopyrite marcasite wurtzite
3	pyrite	marcasite	chalcopyrite sphalerite
4	sphalerite	marcasite	pyrite jarosite wurtzite
5	sphalerite	marcasite, pyrite	jarosite wurtzite
Av.	sphalerite	marcasite pyrite	
Zone B			
7	pyrite	chalcopyrite marcasite	chalcopyrite jarosite sphalerite
8	pyrite, marcasite		chalcopyrite jarosite sphalerite
Av.	pyrite	marcasite	chalcopyrite
Zone C			
9	chalcopyrite	pyrite, sphalerite	marcasite
10	chalcopyrite	pyrite, sphalerite	marcasite pyrite
11	chalcopyrite		sphalerite
Av.	chalcopyrite	pyrite, sphalerite	marcasite
Zone D			
12	sphalerite		chalcopyrite pyrite wurtzite
13	sphalerite		marcasite chalcopyrite
14	sphalerite		pyrite chalcopyrite wurtzite
Av.	sphalerite		chalcopyrite marcasite wurtzite

* Sample G199. The numbers refer to the different points shown on Figure 3a.

Main components: >25 wt.%; Minor component: 10-25 wt.%; Trace component: <10 wt.%. The (Av.) represents the average composition of each zone.

TABLE 2. CHEMICAL COMPOSITION OF THE FOUR GROWTH ZONES*

199 G	SiO ₂ %	Al %	Mn ppm	Fe %	Cu %	Co ppm	Ni %	Zn %	Pb %	Mg ppm	Ag ppm	Cd ppm	Mo ppm
Zone A Youngest outermost rim													
1	1.67	.05	250	32.52	.13	681	.13	8.21	.14	129	127	260	u.d.1
2	3.40	.16	173	24.32	.85	953	.07	29.20	.09	82	195	866	u.d.1.
3	13.45	.10	150	30.63	.34	1365	.04	1.30	.15	103	120	147	280
4	1.13	.05	173	23.83	.12	583	.02	29.67	.15	81	197	387	u.d.1.
5	7.08	.05	104	15.25	.04	494	.02	42.39	.16	81	247	567	u.d.1.
average	5.35	.08	170	25.31	.30	815	.06	22.15	.14	95	177	445	
Zone B First precipitation building the chimney													
6	11.44	.36	170	31.81	.75	2162	.06	4.66	.09	103	163	313	u.d.1.
7	23.53	.36	163	26.00	2.10	2050	.04	1.03	.09	105	123	140	u.d.1.
8	14.06	.05	147	32.15	1.17	839	.03	.90	.08	89	170	u.d.1.	u.d.1.
average	16.34	.26	160	29.99	1.34	1684	.04	2.20	.09	99	152	151	-
Zone C Porous filling of the central channel													
9	25.72	.17	133	20.28	14.19	939	.03	5.33	.09	82	201	173	736
10	4.20	.05	107	25.00	12.53	683	.02	8.30	.07	78	195	203	753
11	4.74	.05	104	23.53	27.01	684	.02	4.34	.07	85	164	144	u.d.1.
average	13.22	.09	115	23.12	17.91	769	.02	5.99	.08	82	187	163	
Zone D Filling of cavities													
12	1.33	.05	120	2.85	.12	530	.02	62.50	.34	73	420	866	u.d.1.
13	.20	.05	104	3.02	.35	307	.01	62.50	.23	78	336	1250	u.d.1.
14	1.0	.05	73	2.29	.31	297	.01	63.08	.25	62	547	1836	u.d.1.
average	.84	.05	99	2.72	.26	378	.01	62.69	.27	71	434	1317	

* The numbers refer to the different points shown in Figure 3a
u.d.1. = under detection limit.

Radiochemical method

For $^{210}\text{Pb}/\text{Pb}$ analysis, about 1 g of sulfide is dissolved in a 7M HNO₃ + 6N HCl mixture spiked with ^{208}Po as a yield tracer. This is heated to dryness and redissolved with HCl to obtain a 0.5N HCl solution. Stable lead is measured on an aliquot of solution by flame atomic-absorption spectrophotometry. From a separate aliquot, ^{210}Po and ^{208}Po were electrochemically deposited onto a silver plate and then measured by alpha spectrometry using a silicon solid-state detector. As the chimney was inactive at the time of sampling, radioactive equilibrium between ^{210}Po and ^{210}Pb has certainly been established, and measurement of ^{210}Po is representative of ^{210}Pb .

After the attack, a residue sometimes remained. Although a HF attack would have solubilized it, we found that the results for several samples following a total attack were the same as those for the leachate. This is because lead is linked mainly to sulfide and not to silicate material. We therefore discontinued the total-digestion procedure. The addition of a ^{208}Po spike takes into account any eventual adsorption of Po isotopes onto the residue.

RESULTS

Mineralogy

Twenty polished sections representing three cross-sections through the upper slice of the chimney were examined by ore microscopy. The mineralogical composition of the four growth zones is given in Table 1; XRD results for 14 samples from the upper slice are given in Table 2, and locations are shown in

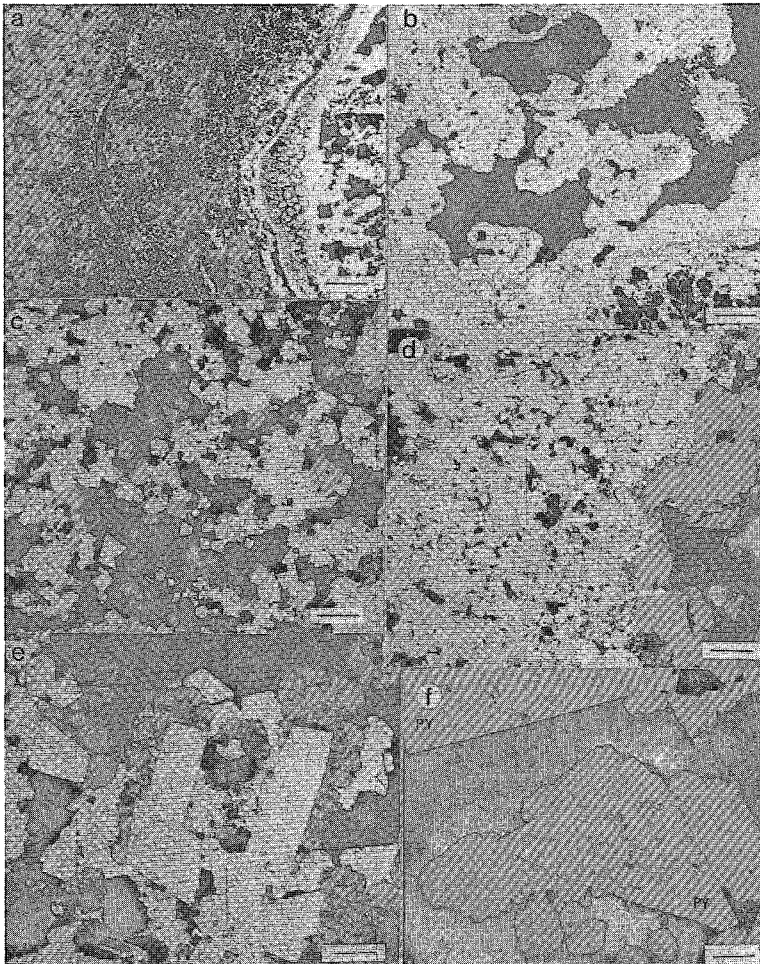


FIG. 4. Photographs of polished sections. (a) Pyrite crust replacement of a worm tube, with pyrite replaced by zinc sulfides. Dendritic zinc sulfides line a cavity. Bar scale: 1 mm. (b) Porous framework of concretionary pyrite coated and partly replaced by crystallized pyrite. Bar scale: 100 μm . (c) Porous framework of pyrite. The presence of euhedral ZnS associated with isocubanite-chalcopyrite suggests recrystallization in response to high-temperature fluids. Bar scale: 100 μm . (d) Chalcopyrite (light grey) replacement of the porous framework of recrystallized pyrite (euhedral) and coated with euhedral ZnS (right side). Bar scale: 80 μm . (e) Elongate pyrite crystals coated with spherulitic ZnS partly replaced by opal (dark thin veins and cores) and coated by late euhedral to spherulitic marcasite. Bar scale: 150 μm . (f) Euhedral pyrite crystal with oriented inclusions of chalcopyrite. Bar scale: 30 μm .

Figure 3a. Mineral associations and textures in the different zones are illustrated in Figures 4 to 6.

Pyrite. Pyrite is the predominant mineral. It is euhedral to cryptocrystalline, spherulitic and concretionary, and displays great differences in reflectivity, zoning, and chemical composition. Concretionary pyrite, which has the lowest reflectivity and highest

porosity, forms crusts that replaced worm tubes, or built loose cellular networks (Figs. 4a,b,c,d) that acted as a framework for later sulfides. Some networks are partly to almost completely recrystallized into euhedral pyrite aggregates (Fig. 4c). Euhedral pyrite is rarely included in colloform pyrite but is often closely associated with marcasite. Skeletal and

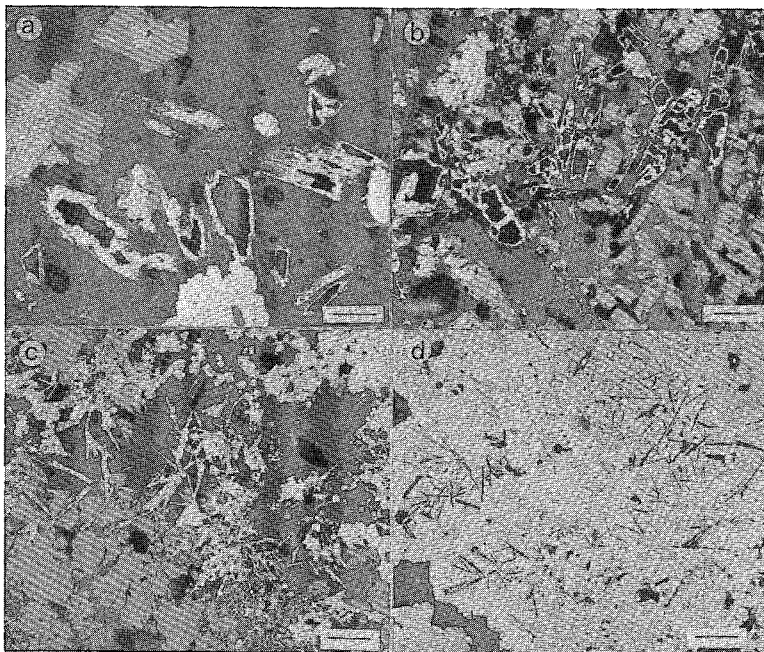


FIG. 5. Photographs of polished sections. (a) Pyrrhotite lamellae partly dissolved (dark cavities) and replaced by opal and marcasite in association with euhedral ZnS containing isocubanite-chalcopyrite and pyrite (euhedral, white). Bar scale: 50 μm . (b) Pyrrhotite lamellae partly dissolved (dark cavities) and replaced by marcasite (unaltered monoclinic pyrrhotite may occur). Bar scale: 100 μm . (c) Porous aggregates of fine-grained pyrrhotite lamellae completely replaced by microcrystalline pyrite and coated by late euhedral ZnS containing cores of isocubanite-chalcopyrite and euhedral pyrite (top right). Bar scale: 120 μm . (d) Extremely fine-grained former pyrrhotite aggregate interpreted as "black smoke" particles replaced by microcrystalline pyrite and coated by coarse-grained marcasite. Bar scale: 25 μm .

unusual elongate crystals of pyrite (Fig. 4e) are locally present. Euhedral pyrite ranges from Co-rich to Co-poor whereas colloform pyrite is depleted in Co (Table 3a). Co-rich euhedral pyrite usually contains inclusions of chalcopyrite (or sometimes pyrrhotite) and is characterized by a slightly higher reflectivity (Fig. 4f). Growth zones in euhedral pyrite are outlined by dissolution surfaces, slight variations in color, and mineral inclusions (Cu or Zn sulfides).

Marcasite. Marcasite is abundant and commonly occurs as spherulites on top of pyrite crystals, as euhedral aggregates with pyrite, or as epitaxial overgrowths on pyrite crystals. Much of the marcasite is late relative to the other sulfides, and may be replaced by opal.

Pyrrhotite. Most pyrrhotite crystals are partly dissolved and partly to completely replaced by pyrite, marcasite and opal (Figs. 5a,b). In the outer chimney walls, monoclinic pyrrhotite is associated with isocubanite-chalcopyrite and zinc sulfides (Fig. 5a).

The stability limit of monoclinic pyrrhotite is 254°C (Craig & Scott 1974) and isocubanite forms by quenching above 210°C (Cabri *et al.* 1973). Therefore, such a mineral association indicates formation between 210 and 254°C. Fine-grained porous aggregates of pyrrhotite completely replaced by microcrystalline pyrite resemble "black smoke" particles described from other EPR deposits (RISE Project Group 1980, Oudin 1981), and thus could represent fossilized smoke particles (Figs. 5c,d).

Chalcopyrite, covellite and idaite. Chalcopyrite is a predominant phase in the central part of the chimney, where it is rarely associated with isocubanite. Two different types of chalcopyrite are recognized. Chalcopyrite I, the most abundant, forms euhedral aggregates that fill cavities lined by Co-bearing pyrite which is extensively replaced (Fig. 6a). Chalcopyrite II, which coats chalcopyrite I, is characterized by an unusual fibrous to microcrystalline texture (Fig. 6b) that may have been inherited through replacement

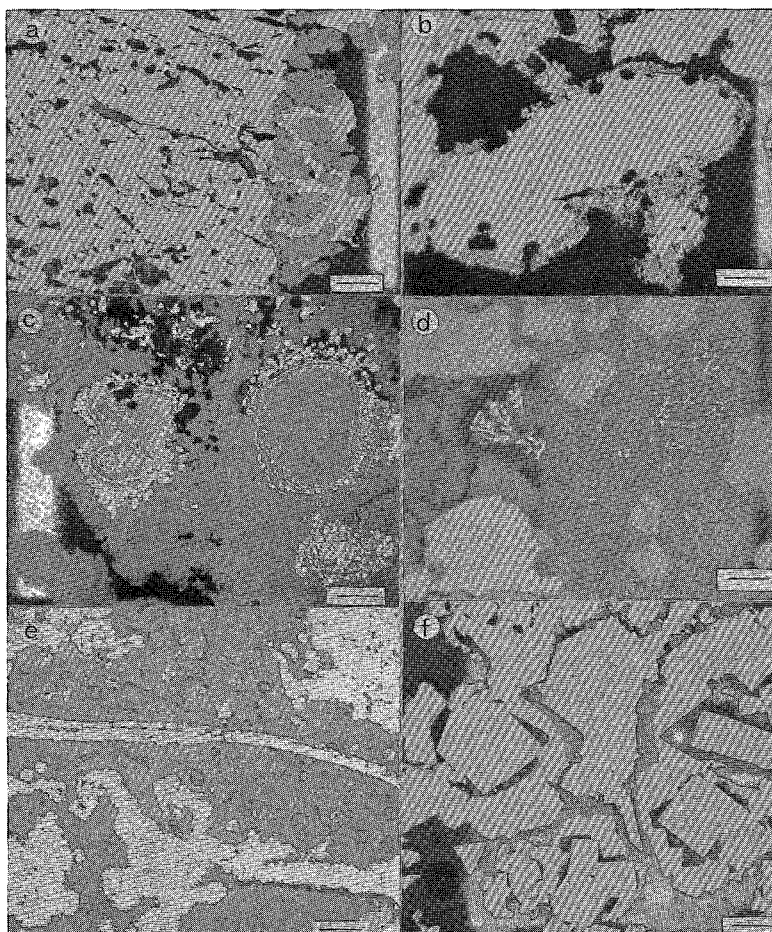


FIG. 6. Photographs of polished sections. (a) Zone D, probably the youngest zone. Central channel is filled with euhedral dendritic zinc sulfide. Elongate chalcopyrite-I crystals initially extended from zone B. Late marcasite coats zone D zinc sulfide and also forms a thin veinlet that cuts the massive chalcopyrite layer. Bar scale: 300 μm . (b) Chalcopyrite-I crystal (light grey) with ZnS inclusions on its outer rim partly replaced by chalcopyrite-II and opal. Fibrous chalcopyrite-II forms a rim on chalcopyrite-I. Bar scale: 30 μm ; oil immersion. (c) Zinc sulfides (dark grey) with concentric chalcopyrite-isocubanite zones from rim of zone A. Oil immersion; bar scale 50 μm . (d) Scanning electron microscope photograph of dendritic galena included in opal associated with pyrite. Bar scale: 40 μm . (e) Spongy aggregate of opal (slightly darker than epoxy resin) on concretionary pyrite crusts. Bar scale: 130 μm . (f) Euhedral pyrite surrounded by chalcopyrite and coated by two generations of ZnS separated by a thin rim of opal followed by late sphalerite. Bar scale: 50 μm .

of covellite. Chalcopyrite II also replaced some small euhedral ZnS grains situated at the edges of large chalcopyrite I crystals. Chalcopyrite II is partly replaced by opal. Microprobe analysis indicates that both chalcopyrite I and II have compositions close to stoichiometry (Table 3b). Rare idaite occurs in chalcopyrite replaced by opal, or in chalcopyrite II.

Isocubanite-chalcopyrite. The isocubanite-chalcopyrite assemblage typical of present-day submarine sulfide deposits is developed mainly in the outermost zone of the chimney. Isocubanite forms euhedral grains with rims and thin oriented lamellae of chalcopyrite. Isocubanite also tends to partly replace euhedral pyrite grains. Some isocubanite con-

TABLE 3a. MICROPROBE ANALYSES OF PYRITE

Grain Anal*.	Co	As	S	Fe	Se	Cu	Ni	Total
Euhedral								
1	.00	.00	52.46	45.02	.03	1.64	.00	99.15
2	.00	.00	52.50	45.08	.00	1.42	.00	99.00
3								
a	1.41	.02	52.87	44.38	.00	.41	.00	99.09
b	.00	.01	52.70	45.52	.00	.74	.00	99.97
c	.84	.00	52.69	44.59	.00	.53	.00	98.65
4								
a	.89	.01	52.93	45.34	.00	.53	.00	99.50
b	1.09	.03	53.43	44.52	.00	.27	.00	99.34
c	.04	.09	52.98	45.48	.00	.13	.00	98.72
5								
6	.46	.17	53.09	44.98	.00	.15	.00	98.85
7	.49	.07	52.47	45.31	.06	.00	.00	98.40
7								
a	1.34	.08	52.76	44.82	.00	.02	.00	99.02
b	.78	.12	53.01	45.48	.00	.00	.00	99.39
c	1.06	.02	52.68	44.82	.00	.02	.00	98.60
d	1.18	.00	52.45	44.61	.00	.00	.00	98.24
e	1.14	.02	53.36	44.99	.00	.00	.00	99.51
8	.00	.00	53.40	45.50	.00	.28	.00	99.18
9	.01	.02	53.09	45.78	.00	.19	.00	99.09
10	.02	.00	53.21	45.57	.00	.00	.00	98.80
11	.60	.10	53.28	44.97	.00	.54	.00	99.49
12	.86	.00	53.10	44.85	.00	.12	.00	98.93
13	.79	.05	52.86	45.21	.00	.17	.00	99.08
14	.07	.05	52.99	45.90	.00	.00	.00	99.01
15	.53	.06	52.63	45.59	.00	.00	.00	98.81
16	.14	.32	52.86	45.79	.00	.00	.00	99.11
Colloform								
17	.02	.03	53.26	46.39	.00	.17	.00	99.70
18	.00	.00	53.45	45.82	.00	.00	.00	99.27
19	.01	.00	52.60	46.29	.00	.00	.00	98.90

* Analysis of three separate grains are given in rows 3-5, 6-8 and 11-15 respectively.

tains pyrrhotite inclusions, and some is locally associated with pyrrhotite lamellae and zinc sulfides. Small cavities are lined by isocubanite-chalcocopyrite and zinc sulfides.

Zinc sulfides. Zinc sulfides are abundant in zones A and D, where they form colloform crusts, spherulites, and dendritic assemblages in cavities. The sulfides also occur as euhedra, some of which have hexagonal outlines suggestive of wurtzite. Because wurtzite and sphalerite were not distinguishable in polished section, the general term zinc sulfide is used here. Minute to large inclusions of chalcocopyrite and isocubanite commonly delineate Zn sulfide growth zones; the inclusions formed either on the surfaces of growing crystals or by later selective replacement (Fig. 6c). The wide range of internal reflection colors suggests that the iron content of different zinc sulfide phases is highly variable. Late euhedral to predominantly dendritic zinc sulfides which coat chalcocopyrite-lined cavities in the central part of the chimney (Fig. 6a) have Fe contents of <2.6 wt. % (Table 3c).

Galena. Galena is very scarce and can be overlooked easily because it occurs as extremely fine-grained dendrites or skeletal crystals. It is included in opal in one occurrence in zone B (Fig. 6d).

Opal. Opal is relatively abundant in zone B, where it forms fibrous and spongy aggregates (Fig. 6e). Opal coated and replaced all the other sulfides. It

TABLE 3b. MICROPROBE ANALYSES OF CHALCOCOPYRITE

	Cu	Se	S	Fe	Zn	Total
Chalcocopyrite I						
1	34.09	.00	34.51	30.79	.01	99.40
2	34.17	.00	34.73	30.91	.00	99.81
3	33.71	.05	34.66	31.18	.00	99.60
4	33.85	.00	34.68	30.76	.00	99.29
5	34.09	.04	35.02	30.84	.00	99.99
6	33.64	.00	34.89	20.87	.00	99.40
7	33.48	.00	34.41	30.97	.00	98.86
8	33.82	.00	35.01	31.24	.00	100.07
9	33.32	.04	34.97	30.79	.00	99.12
10	33.64	.00	34.73	30.13	.00	98.50
11	33.84	.00	34.53	30.91	.00	99.28
12	33.58	.00	34.53	31.04	.00	99.15
13	33.99	.00	34.69	30.40	.03	99.11
14	33.90	.23	34.64	30.92	.06	99.75
15	33.56	.00	34.62	30.71	.03	98.92
16	33.69	.00	34.60	30.70	.00	98.99
Mean						
17	33.77	.00	34.70	30.82	.00	99.29
Chalcocopyrite II						
18	34.54	.00	34.04	30.36	.00	98.94
19	34.42	.00	34.44	30.10	.00	98.96
20	34.31	.00	34.59	30.33	.00	99.29
21	34.26	.06	34.64	30.67	.00	99.63
22	33.57	.00	34.75	30.72	.00	99.04

Compositions 1 to 16 are for chalcocopyrite I in cavities in zone C, analyzed at intervals of 200 μ m across the chalcocopyrite layer. Compositions 18 to 22 are for chalcocopyrite II.

TABLE 3c. MICROPROBE ANALYSES OF DENDRITIC SPHALERITE FROM THE CENTRAL PART OF THE CHIMNEY

	S	Fe	Cd	Zn	Mn	Cu	Total
1	32.35	2.61	.13	63.20	.00	.05	98.34
2	33.14	.96	.00	65.24	.00	.00	99.34
3	37.79	1.23	.25	63.80	.00	.40	98.47
4	32.79	2.11	.12	63.28	.00	.19	98.49
5	33.41	1.66	.12	62.41	.00	.47	98.07

often forms a thin film separating two generations of the same sulfide (Fig. 6f). Much of the opal contains a slightly more reflective phase with a lower polishing hardness which has a relatively high Al content, at least 1% as indicated by SEM analysis. A Si-Al-bearing phase with an amorphous X-ray pattern also has been reported for samples from 21°N EPR (Oudin 1981).

Other phases. Minor amounts of goethite replaced colloform pyrite crusts which were in contact with seawater. In the same zone, a zinc sulfate occurs on zinc sulfides. Jarosite also was identified by X-ray diffraction. These phases probably form through alteration of sulfides by cold seawater.

Radiochronology

Although the $^{210}\text{Pb}/\text{Pb}$ initial ratio must depend on the U/Pb ratio of the basalts, the ratio probably varies from one hydrothermal system to another depending on water-rock ratio, previous rock alteration, and residence time of the fluid within the system (Turekian *et al.* 1979, Krishnaswami & Turek-

ian 1982, Kadko *et al.* 1985). To obtain meaningful data at a particular locality, it is necessary to know the ratio at the onset of precipitation. The first such measurements were by Finkel *et al.* (1980) who determined this ratio in the sulfide particles filtered from the plume of a black smoker at 21°N, EPR. They found a value of 1.8 dpm/μg of stable lead, from which they concluded that ²¹⁰Pb (as well as stable Pb) was derived from basalt alteration, with no seawater contribution. Using this value, Lalou & Brichet (1981, 1982) calculated ages of 23 ± 10 to 61 ± 4 years for sulfide chimneys from the 21°N hydrothermal field. At 12°50'N on the EPR, a value of 0.6 dpm/μg Pb was obtained (and was confirmed two years later from particles from another active vent in the same hydrothermal area). The calculated ages for the chimneys of this area cover a time span of about 80 years (Lalou *et al.* 1985). It seems, therefore, that although the ²¹⁰Pb/Pb ratio does not change appreciably with time in a given field, each field may have a characteristic initial ratio. At 18°S, the two chimneys at the sample locality were not hydrothermally active, which required us to use the highest ratio found in the chimney as a relative "zero" point. All other lower ratios then may be used to calculate ages relative to this point.

From Table 4, it can be seen that the highest ²¹⁰Pb/Pb ratio is 0.111 ± 0.008 at point 2. This is actually the lowest "initial ratio" yet reported, and

is notably less than the 0.56 value given by Kadko *et al.* (1985) for sulfides on the Juan de Fuca Ridge. The difference in ages between this arbitrary zero point and the oldest one (point 16) is about 80 years, which is very similar to the true ages of chimneys in other hydrothermal fields (Lalou & Brichet 1982, Lalou *et al.* 1985). This may reflect the fact that the extremely high heat flow at chimneys requires that vent activity be highly episodic and of short overall duration (on the order of 100 years; Macdonald *et al.* 1980). If instead of 0.111 we took the initial ratio as 0.6 (the value for vents on the EPR at 12°50'N), this would result in ages about 50 years older, from 50 to 130 years.

In terms of chimney zonation (Fig. 3b), five samples from zone A have relative ages of 0, 7, 6, 35 and 1.8 years. In zone B, three samples span 63 to 82 years. A sample from inner zone C has a relative age of 13 years, and two samples from inner zone C' have apparent ages of 22 and 14 years. Zone D, the dendritic filling in the upper slice (point d, Fig. 3a) has an apparent age of 10 years.

Except for point 9 (35 years), which may have resulted from a sampling mixture of the inner and outer walls, the results of age dating give a coherent temporal frame to the buildup of the chimney. Growth began around 80 years ago, as two conduits. About 60 years later, the hydrothermal activity ceased and the two conduits were plugged. More recently, and perhaps always active, the hydrothermal fluid had to diffuse from the base of the edifice, forming the very recent outer zones A and D.

TABLE 4. RADIOCHRONOLOGICAL RESULTS

Sample n**	Pb (ppm)	²¹⁰ Pb** (dpm/g)	²¹⁰ Pb/Pb	Relative ages (years)
Zone B				
11	375±18	4.1±0.4	.011 ± .001	73 ± 3.5
15	875±44	13.1±0.8	.015 ± .001	63 ± 2.5
16	630±30	5.3±0.3	.0084±.0006	82 ± 2
Zone C				
1	360±18	25.8±1.6	.072 ± .006	13 ± 2.5
Zone C'				
12	215±10	11.9±0.7	.055 ± .004	22 ± 2
17	345±17	24.6±1.8	.071 ± .006	14 ± 2.5
Zone A				
2	505±25	56.2±2.9	.111 ± .008	0***
3	240±12	21.3±1.3	.089 ± .007	7 ± 2.5
4	510±25	46.9±3.3	.092 ± .008	6 ± 2.5
9	645±32	23.9±1.5	.037 ± .003	35 ± 2.5
13	360±18	37.8±2.1	.105 ± .008	1.8±2.4
Zone D (dendritic growth)				
d	1647±17	133 ± 8	.081 ± .006	10 ± 2.5

*Sample number refers to the points shown in Fig. 3b; sample d location is given in Fig. 3a.

**²¹⁰Pb activities have been recalculated at the sampling date (Jan. 5, 1986).

***Reference ratio

Precision on stable lead measurements is ±5%.

Errors on ²¹⁰Pb are ±1σ counting statistics.

DISCUSSION

Growth model for 18°25'S chimney

On the basis of mineralogical zonation, chemical data, and relative age determinations, the following schematic growth history of the chimney may be advanced. The history is better described in terms of hydrothermal stages because, although one or two predominant hydrothermal stages control the formation of each mineral zone, the zones are modified by the successive hydrothermal events as indicated by mineralogical studies and age determinations.

STAGE I: high-temperature event. The primitive chimney structure started forming when high-temperature fluid, emitted at high speed on the seafloor, deposited a fine-grained assemblage of pyrrhotite crystals (probably associated with other minor sulfides and anhydrite). This event was short-lived or poorly preserved (or both), and was fossilized during the subsequent deposition of pyrite.

STAGE II. A porous aggregate of predominantly concretionary pyrite and marcasite followed by opal then replaced the primitive structure. The cryptocrystalline texture of pyrite, which partly forms the cellular network, and the paragenetic succession established on 21°N samples by Oudin (1981), sug-

gest that this structure was formed by low-temperature fluids as a result of supersaturation. The structure, best represented by zone B, was formed at least 80 years earlier than the youngest chimney sample. Galena is present in opal. As the measured age of zone B is probably that of galena, the main Pb carrier, the porous pyrite and marcasite aggregate may have begun to form earlier than its apparent age of 80 years. The three different age values, spanning 63–82 years, may reflect either different hydrothermal events early in chimney formation, or a mixture of material of different ages in the analyzed samples.

This mineral structure was again transformed by later fluid circulation. During this low-temperature event the surface of the chimney was colonized by worms, indicating that optimum conditions existed for these organisms during or before mineralization. The chimney must have been near its definitive width because subsequent mineral precipitates formed mainly within the porous structure.

STAGE III: high-temperature event. A new phase of hydrothermal activity 55–70 years later produced Cu-rich zone C by partly filling the central conduit of the chimney. Precipitation of chalcopyrite I and Co-bearing pyrite was followed by minor amounts of Zn sulfides. Covellite (or idaite) formed at lower temperatures, either during the waning of hydrothermal activity or by seawater alteration, and was replaced by chalcopyrite II. Chalcopyrite in the central part of the chimney has a near-stoichiometric composition, typical of relatively thick chimney walls (Oudin 1981). This contrasts with the zoned Fe–S-rich chalcopyrite in thin (up to 1 cm) chimney walls of black smokers at 21°N and 13°N on the EPR (Oudin 1981, 1987, Lafitte *et al.* 1984). The latter chalcopyrite composition may reflect extreme thermal and chemical gradients in thin chimney walls at sulfur fugacities too high for isocubanite deposition. The growth of large crystals of near-stoichiometric composition in the central part of the 18°25'S chimney suggests that chalcopyrite may have grown in near-equilibrium with the hydrothermal fluid. Zone C averages 18% Cu and 13% SiO₂ (SiO₂ varies from 5 to 26%). The silica occurs as opal-A. The Zn content (~6%) is somewhat higher than in zone B.

Cobalt-rich pyrite (mainly in zones B and C), the copper and zinc iron sulfides observed in zone B (averaging 1.3% Cu and 2.2% Zn), and the monoclinic pyrrhotite – isocubanite – chalcopyrite and euhedral ZnS assemblage in zone A may also have formed during this third hydrothermal event. The concretionary pyrite structure formed during stage II also may have recrystallized.

The increased crystallinity of pyrite, and the increased chalcopyrite/isocubanite ratio towards the center of the chimney, are probably the result of gradients across the chimney wall between seawater and

high-temperature hydrothermal fluid during stage III. In the central part of the chimney, which was isolated from seawater by the older chimney wall, chalcopyrite alone was precipitated, while the quenched pyrrhotite–isocubanite–chalcopyrite and ZnS assemblage was precipitated in the inner part of zone A.

STAGE IV: low-temperature event. A less intense reactivation of the system occurred 0–10 years later. Sealing of the conduit hindered direct discharge of hydrothermal solutions, which may have forced the solutions to exit through the base of the chimney and migrate upward along the chimney exterior during stage IV. Sea-bottom television and photographic observations in this area have shown that this mode of discharge is typical of large, well-developed chimneys (Marchig, own shipboard observations). Dendritic sphalerite lines worm tubes in zone A, and also lines the last small cavities in the feeder channel of zone C. One ²¹⁰Pb/Pb measurement of dendritic sphalerite from the upper slice of the chimney gave an apparent age of 10 years. Some of the pyrite may have been deposited in zone A during stage IV. During this stage, the overall width of the chimney was probably increased slightly. Zone D is nearly pure sphalerite enriched in traces of Pb, Cd and Ag relative to sphalerite from other zones. However, pyrite and marcasite occur only in trace amounts. Lower porosity and clogging of the central conduit limited diffusive fluid flow through the walls, and mineral precipitation in zone B.

STAGE V: seawater alteration. When the hydrothermal activity ceased, the massive sulfide chimney was exposed to seawater alteration. Minerals such as goethite and jarosite were formed by oxidation of iron sulfides by reaction with seawater.

COMPARISON WITH OTHER EPR CHIMNEY GROWTH MODELS

The mineral associations and textures at 18°25'S are generally similar to those of other deposits described from sediment-barren segments of the EPR at 21°N (Hékinian *et al.* 1980, Haymon & Kastner 1981, Oudin 1981, 1982, 1983, Styrut *et al.* 1981, Goldfarb *et al.* 1983, Zierenberg *et al.* 1984), at 13°N (Lafitte *et al.* 1984, Hékinian & Fouquet 1985, Graham *et al.* 1988) on the Juan de Fuca Ridge (Koski *et al.* 1984, Paradis *et al.* 1988), on the Endeavor Ridge (Tivey & Delaney 1986), and in the South Pacific, East Pacific Rise and Galapagos Ridge (Oudin 1982, Tufar *et al.* 1984, 1985, 1986).

The main difference in mineral assemblages is the absence of anhydrite and barite. Anhydrite forms by mixing of Ca-rich hot hydrothermal fluid and SO₄-rich seawater at temperatures above 140°C (Haymon & Kastner 1981, Oudin 1981). Large amounts of anhydrite are not expected in our chim-

ney, where high-temperature mineral associations such as isocubanite–chalcopyrite–pyrrhotite or chalcopyrite were deposited within the chimney walls wherein only limited amounts of fluid mixing could occur. No replacement textures of anhydrite by sulfides or opal, which have been described in other EPR samples (Oudin 1981, Haymon 1983, Tivey & Delaney 1986, Paradis *et al.* 1988) have been observed in our chimney. Anhydrite has a retrograde solubility at low temperatures. Therefore, anhydrite which may also have been associated with early “black smoke” particles such as pyrrhotite would have been dissolved during pyrrhotite replacement by microcrystalline pyrite; as our chimney was inactive, later anhydrite also could have dissolved. For the same reasons, anhydrite is not usually observed in 21°N sulfide mounds (Oudin 1981, Haymon & Kastner 1981, Styrts *et al.* 1981), in Juan de Fuca samples (Koski *et al.* 1984), or in large sulfide samples from Endeavor Ridge (Tivey & Delaney 1986).

Although barite is a common accessory mineral in the other deposits listed above, it was not identified in our chimney. Barite is missing or extremely rare also in other massive sulfide samples from EPR 18°S to 21°S (scientific report of SO 40 cruise), the main accessory mineral being amorphous silica.

Chimney growth models have generally been based on the study of high-temperature, thin (average 1 cm) chimney walls having an inner wall dominated by Cu or Zn sulfides (or both), and an outer wall usually dominated by anhydrite (21°N chimney growth model; Oudin 1981, Haymon 1983, Goldfarb *et al.* 1983, Paradis *et al.* 1988). All authors emphasize the importance of the numerous mineral transformations (dissolution, replacement) as well as the steep physical and chemical gradients which control the construction of the chimney walls and their zonations. Graham *et al.* (1988) describe larger chimney samples from 11°N and 13°N with similar zonation and suggest that the relative rates of nucleation of the different phases are probably also important factors which contribute to the mineral-zone formation. The mineral zonations in the 18°25'S chimney are probably controlled by the same processes, although a change in fluid chemistry can also be considered. Our mineralogical observations suggest that during stage III, a gradient was formed between the outer wall and the inner conduit. If chalcopyrite in the inner conduit was formed at 300–350°C, as in other EPR black smokers (Oudin 1981, Haymon & Kastner 1981, Styrts *et al.* 1981), then both the 15-cm-thick wall of 18°25'S chimney and the thin (~1 cm) black-smoker walls at 21°N have been subjected to similar temperature variations (up to 350°C). The pyrite crystallinity and the isocubanite–chalcopyrite ratio variations are progressive, suggesting progressive temperature gradients in the 18°25'S chimney. Post-precipitation processes such as dissolution and

replacement are not as intense in 18°25'S chimney; instead, recrystallization is particularly well-developed. As a result, many of the primary features in the 18°25'S chimney are better preserved than in 21°N chimneys.

Tivey & Delaney (1986) explained the formation of large, complex massive sulfide (incomplete) structures from Endeavor Ridge by the combination of two distinct processes: several 21°N-like chimneys were formed and sealed during several flow redirections, and were consolidated by amorphous silica deposition during diffuse hydrothermal flow. Our 18°25'S chimney shows no evidence of high-temperature chalcopyrite-dominated chimney walls which would have formed at the hydrothermal fluid–seawater interface; on the contrary, the chalcopyrite-dominated zone must have formed inside the edifice as indicated by its relative age and stoichiometric composition which do not indicate quenching by seawater. The model developed by Koski *et al.* (1984) for a layered massive sulfide sample from Juan de Fuca Ridge suggests that an initial low-temperature concretionary deposit of Fe and Zn sulfides later inhibits mixing of seawater and hydrothermal fluids, thereby allowing precipitation of higher temperature mineral assemblages inside the structure; rupture of the original walls allows fluids to escape and outward growth of the wall. This model is closer to the model we are proposing for our 18°25'S chimney, as insulation of the hydrothermal fluid is due to the presence of an early, low-temperature wall.

CONCLUSIONS

Our model of chimney growth, based on submarine observation, chemical and mineralogical studies, and ²¹⁰Pb/Pb age determinations, suggests the succession of four main hydrothermal events during a period of over 80 years. The hydrothermal activity is either a continuous process with cyclic periods of peak hydrothermal activity, or is a discontinuous process (episodic hydrothermal activity) which could be controlled by tectonic and volcanic activity.

The primitive chimney structure is built at the seawater – hydrothermal fluid interface. This early wall partly insulates later fluids: the fluid deposits a massive chalcopyrite layer on the highly porous inner structure and also diffuses through the porous walls, overprinting discrete mineral zonations and recrystallization gradients. Reduction of the porosity, and the filling of the large cavities of the inner structure, eventually force the fluid to break through at the base of the chimney and to flow upward along the surface of the chimney outer wall.

ACKNOWLEDGEMENTS

V.M. and H.R. thank the German Ministry of

Research and Technology for the financial support of the scientific cruise. C.L. and E.B. acknowledge financial support from the French CNRS and CEA (CFR contribution n° 908). E.O. thanks G. Scolari from the BRGM scientific direction, who partly supported this study. We thank two anonymous referees for constructive criticisms.

REFERENCES

- BÄCKER, H., LANGE, J. & MARCHIG, V. (1985): Hydrothermal activity and sulphide formation in axial valleys of the East Pacific Rise Crest between 18 and 22°S. *Earth Planet. Sci. Lett.* **72**, 9-22.
- BECKER, K. & LONSDALE, P.F. (1985): Hydrothermal plumes, hot springs, and conductive heat flow in the Southern trough of Guaymas Basin. *Earth Planet. Sci. Lett.* **73**, 211-225.
- CABRI, L.J., HALL, S.R., SZYMAŃSKI, J.T. & STEWART, J.M. (1973): On the transformation of cubanite. *Can. Mineral.* **12**, 33-38.
- CORLISS, J.B. & BALLARD, R.D. (1977): Oases of life in the cold abyss. *J. Nat. Geogr. Soc.* **152**, 441-453.
- CRAIG, J.R. & SCOTT, S.D. (1974): Sulfide phase equilibria. *Mineral. Soc. Amer. Short Course Notes* **1**.
- EDMOND, J.M., MEASURES, C., MCDUFF, R.E., CHAN, L.H., COLLIER, R., GRANT, B., GORDON, L.I. & CORLISS, J.B. (1979): Ridge crest hydrothermal activity and the balance of the major and minor elements in the ocean: the Galapagos data. *Earth Planet. Sci. Lett.* **46**, 1-8.
- FINKEL, R.C., MACDOUGALL, J.D. & CHUNG, Y.C. (1980): Sulfide precipitates at 21°N on the East Pacific Rise: ²²⁶Ra, ²¹⁰Pb and ²¹⁰Po. *Geophys. Res. Lett.* **7**, 685-688.
- FRANCHETEAU, J., NEEDHAM, H., CHOUKROUNE, P., SIGURET, M., BALLARD, R., FOX, P., NORMARK, W., CARRANZA, A., CORDOBA, D., GUERRERO, V., RANGIN, C., BOUGAULT, H., CAMBON, P. & HÉKINIAN, R. (1979): Massive deep-sea sulfide ore deposits discovered by submersible on the East Pacific Rise: Project RITA, 21°N. *Nature* **277**, 523-528.
- _____ & BALLARD, R.D. (1983): The East Pacific Rise near 21°N, 13°N and 20°S: inferences for along-strike variability of axial processes of the Mid-Ocean Ridge. *Earth Planet. Sci. Lett.* **64**, 93-116.
- GOLDFARB, M.S., CONVERSE, R.D., HOLLAND, H.D. & EDMOND, J.M. (1983): The genesis of hot spring deposits on the East Pacific Rise, 21°N. *Econ. Geol. Monogr.* **5**, 184-197.
- GRAHAM, U.M., BLUTH, G.J. & OHMOTO, H. (1988): Sulfide-sulfate chimneys on the East Pacific Rise, 11° and 13°N latitudes. Part I: mineralogy and paragenesis. *Can. Mineral.* **26**, 487-504.
- HAYMON, R.M. (1983): Growth history of hydrothermal black smoker chimneys. *Nature* **301**, 695-698.
- _____ & KASTNER, M. (1981): Hot spring deposits on the East Pacific Rise at 21°N: preliminary description of mineralogy and genesis. *Earth Planet. Sci. Lett.* **53**, 363-381.
- HÉKINIAN, R. & FOUQUET, Y. (1985): Volcanism and metallogenesis of axial and offaxial structures on the East Pacific Rise near 13°N. *Econ. Geol.* **80**, 221-249.
- _____, FEVRIER, M., BISCHOFF, J.L., PICOT, P. & SHANKS, W.C., III (1980): Sulfide deposits from the East Pacific Rise near 21°N. *Science* **207**, 1433-1444.
- _____, FRANCHETEAU, J., RENARD, V., BALLARD, R.D., CHOUKROUNE, P., CHEMINEE, J.L., ALBAREDE, F., MINSTER, J.F., CHARLOU, J.L., MARTY, J.C. & BOULEGUE, J. (1983): Intense hydrothermal activity at the axis of the East Pacific Rise near 13°N; submersible witnesses the growth of sulfide chimney. *Mar. Geophys. Res.* **6**, 1-14.
- KADKO, D., KOSKI, R., TATSUMOTO, M. & BOUSE, R. (1985): An estimate of hydrothermal fluid residence times and vent chimney growth rates based on ²¹⁰Pb/Pb ratios and mineralogic studies of sulfides dredged from the Juan de Fuca Ridge. *Earth Planet. Sci. Lett.* **76**, 35-44.
- KOSKI, R.A., CLAGUE, D.A. & OUDIN, E. (1984): Mineralogy and chemistry of massive sulfide deposits from the Juan de Fuca Ridge. *Geol. Soc. Amer. Bull.* **95**, 930-945.
- KRISHNASWAMI, S. & TUREKIAN, K.K. (1982): ²³⁸U, ²²⁶Ra and ²¹⁰Pb in some vent waters from the Galapagos Spreading Center. *Geophys. Res. Lett.* **9**, 827-830.
- LAFFITE, M., MAURY, R. & PERSEIL, E.A. (1984): Analyse minéralogique de cheminées à sulfures de la dorsale Est Pacifique (13°N). *Mineral. Deposita* **19**, 274-282.
- LALOU, C. & BRICHET, E. (1981): Possibilité de datation des dépôts de sulfures métalliques hydrothermaux sous marins par les descendants à vie courte de l'uranium et du thorium. *C.R. Acad. Sci. Paris, Série II*, **293**, 821-826.
- _____ & _____ (1982): Age and implication of East Pacific Rise sulphide deposits at 21°N. *Nature* **300**, 169-171.
- _____, _____ & HÉKINIAN, R. (1985): Age dating of sulfide deposits from axial and off-axial structures of the East Pacific Rise near 12°50'N. *Earth Planet. Sci. Lett.* **75**, 59-71.
- LONSDALE, P.F., BISCHOFF, J.L., BURNS, V.M., KASTNER, M. & SWEENEY, R.E. (1980): A high temperature hydrothermal deposit in the seabed at a Gulf of California spreading center. *Earth Planet. Sci. Lett.* **49**, 8-20.
- MACDONALD, K.C., BECKER, K., SPIESS, F.N. & BALLARD, R.D. (1980): Hydrothermal heat flux of the "black smoker" vents on the East Pacific Rise. *Earth Planet. Sci. Lett.* **48**, 1-7.
- MARCHIG, V., GUNDLACH, H. & THE SHIPBOARD SCIENTIFIC PARTY (1987): Ore formation of rapidly diverging plate margins. Results of cruise GEOMETEP 4. *BGR-Circular* **4**, 3-22.
- _____, WILKE, M. & HOLLER, G. (1988): New discoveries of massive sulfides on the East Pacific Rise. In *Hydrothermal Activity and Metalliferous Sediments on the Ocean Floor* (P. Stoffers, ed.). Strasbourg, 1987. *Marine Geol.*, Special Issue (in press).
- NORMARK, W.R., MORTON, J.L., KOSKI, R.A., CLAGUE, D.A. & DELANEY, J.R. (1983): Active hydrothermal vents and sulfide deposits on the southern Juan de Fuca Ridge. *Geology* **11**, 158-163.

- OUDIN, E. (1981): Étude minéralogique et géochimique des dépôts sulfurés sous-marins actuels de la ride Est Pacifique (21°N) Campagne RISE. *Doc. BRGM* **25**.
 — (1982): Mineralogical study of hydrothermal sulfides collected on the Galapagos Rift at 0°45'N: a comparison with other rift sulfides. *Rapport BRGM* **82**, SGN, 841 MGA.
 — (1983): Hydrothermal sulfide deposits of the East Pacific Rise (21°N) I. Descriptive mineralogy. *Mar. Mining* **4**, 39-72.
 — (1987): Trace elements and precious metal concentration in East Pacific Rise, Cyprus and Red Sea submarine sulfide deposits. In *Marine Minerals* (P. Teleki, M.R. Dobson, J.R. Moore & U. von Stackelberg, eds.). *NATO ASI Series C*, **194**, 349-362. D. Reidel Pub. Co., Dordrecht, Holland.
- PARADIS, S., JONASSON, I.R., LE CHEMINANT, G.M. & WATKINSON, D.H. (1988): Two zinc-rich chimneys from the Plume Site, southern Juan de Fuca Ridge. *Can. Mineral.* **26**, 637-654.
- RENARD, V., HÉKINIAN, R., FRANCHETEAU, J., BALLARD, R.D. & BÄCKER, H. (1985): Submersible observations at the axis of the ultra-fast-spreading East Pacific Rise (17°30' to 21°30' S). *Earth Planet. Sci. Lett.* **75**, 339-353.
- RISE PROJECT GROUP (1980): East Pacific Rise: hot springs and geophysical experiments. *Science* **207**, 1421-1433.
- RONA, P.A., KLINKHAMMER, G., NELSON, T.A., TREFRY, J.H. & ELDERFIELD, H. (1986): Black smokers, massive sulphides and vent biota at the Mid-Atlantic Ridge. *Nature* **321**, 33-37.
- STYRT, M.M., BRACKMANN, A.J., HOLLAND, H.D., CLARCK, B.C., PISUTHA-ARNOND, V., ELDRIDGE, C.S. & OHMOTO, H. (1981): The mineralogy and the isotopic composition of sulphur in hydrothermal sulphide/sulphate deposits on the East Pacific Rise, 21°N latitude. *Earth Planet. Sci. Lett.* **53**, 382-390.
- TIVEY, M.K. & DELANEY, J.R. (1986): Growth of large sulfide structures on the Endeavour segment of the Juan de Fuca Ridge. *Earth Planet. Sci. Lett.* **77**, 303-317.
- TUFAR, W., GUNDLACH, H. & MARCHIG, V. (1984): Zur Erzparagenese rezenter Sulfid-Vorkommen aus dem südlichen Pazifik. *Mitt. öster. Geol. Ges.* **77**, 185-245.
- , — & — (1985): Ore paragenesis of recent sulfide formations from the East Pacific Rise. *Monograph Series on Mineral Deposits* **25**, 75-93 (Geobrüder Bornaege, eds.). Berlin, Stuttgart.
- , TUFAR, E. & LANGE, J. (1986): Ore paragenesis of recent hydrothermal deposits at the Cocos-Nazca plate boundary (Galapagos Rift) at 85°51' and 85°55' W: complex massive sulfide mineralizations, non sulfidic mineralizations and mineralized basalts. *Geol. Rundschau* **75**, 829-861.
- TUREKIAN, K.K., COCHRAN, J.K. & NOZAKI, Y. (1979): Growth rate of a clam from the Galapagos Rise hot spring field using natural radionuclide ratios. *Nature* **280**, 385-387.
- ZIERENBERG, R.A., SHANKS, W.C., III & BISCHOFF, J.L. (1984): Massive sulfide deposits at 21°N, East Pacific Rise: Chemical composition, stable isotopes, and phase equilibria. *Geol. Soc. Amer. Bull.* **95**, 922-929.

Received June 25, 1987; revised manuscript accepted June 16, 1988.